

# Hydrodynamic arrest of a flat body moving towards a parallel surface at arbitrary Reynolds number

By C. J. LAWRENCE† AND S. WEINBAUM

Department of Mechanical Engineering, The City College of the City University of New York,  
New York, NY 10031, USA

(Received 16 September 1985 and in revised form 20 October 1986)

The motion of a flat body towards a parallel plane surface in incompressible fluid is considered both in the presence and absence of an applied force for a non-vanishing initial velocity. In the inviscid limit, a first integral of the equations is obtained and analytic solutions are presented for the cases of finite body inertia with zero applied force and finite applied force with negligible body inertia. In the former case when the ratio of body inertia to fluid inertia is large, a singular behaviour is observed in the arrest of the body before impact wherein the time-dependent pressure and radial velocity of the fluid exhibit a sharp peak and there is a large transfer of kinetic energy from the body to the thin fluid layer. For a real fluid, a general procedure is described to obtain solutions at arbitrary Reynolds number for naturally occurring initial velocity conditions. Solutions to the full Navier–Stokes equations are obtained for an arbitrary Reynolds number based on gap height which are valid provided the flow remains laminar and the gap height is small. In general, the equations of motion of the body and fluid are both dynamically and kinematically coupled. The dynamic coupling, however, is removed when the body inertia is neglected. In particular, the cases of hydrodynamic arrest with zero applied force, and draining of the fluid under a constant applied force are considered. The natural initial conditions lead to a new exact similarity solution of the Navier–Stokes equations which is valid for an instantaneous time-dependent  $Re$  based on gap height of greater than approximately 100, wherein the top and bottom boundary layers remain distinct. The longer time portions of the motion and the final arrest are described by a numerical calculation for intermediate Reynolds number and a low-Reynolds-number analysis.

---

## 1. Introduction

The draining of a fluid layer in the hydrodynamic collision of an object with a boundary underlies a diversity of physical phenomena associated with filtration, coagulation and biological applications. In virtually all of the studies to date, these interactions have been treated either in the viscosity-dominated limit, where particle and fluid inertial effects can be ignored, or in the inviscid limit where all real-fluid effects are omitted. The vast majority of analyses in the viscous limit have been based on either the quasi-steady Stokes equation in the limit of zero Reynolds number or lubricating-layer theories where the Reynolds number based on gap height is small and all inertial effects in the fluid layer can be neglected. The latter

† Present address: Department of Theoretical and Applied Mechanics, University of Illinois at Urbana-Champaign, Urbana, IL 61801, USA.

approximation has been used in the recent theory of Davis, Serayssol & Hinch (1986), the first analysis that attempts to address the difficult problem of the elasto-hydrodynamic collision and rebound of solid particles from a wall in a viscous fluid.

Depending on the initial velocity of the particle, the Reynolds number based on the instantaneous height of the fluid gap can take very large values where inertial effects are dominant or very small values during collision when the fluid gap is very narrow. The problem of the near-collision approach, however, has an important simplification in that the boundary geometry in the region of near contact will be nearly parallel, at least for a blunt object, and the boundaries may be flattened by elastic deformation. Therefore, important insights can first be obtained by examining the fully nonlinear problem for the simple inelastic parallel wall geometry. For mathematical simplicity, we consider an object with a flat circular bottom moving towards a parallel plane surface, as shown in figure 1, and we will assume that the initial gap height  $h_0$  is much smaller than the disk radius  $a$ . The fluid motion in the gap can be visualized as a time-dependent axisymmetric double stagnation-point flow.

The problem described has already been studied in the case where the body is dropped from rest near the plane and falls under the action of a constant normal force. (Weinbaum, Lawrence & Kuang 1985; Lawrence, Kuang & Weinbaum, 1985. These papers will hereinafter be referred to as WLK 1 and LKW 2.) In the present paper, we are interested primarily in the motion of a body approaching from far away under the influence of its own inertia and fluid inertia. For a viscous fluid, there will be dissipation of energy and, in the absence of elasticity or an applied force, the body will come to rest without recoil at some distance from the plane. In WLK 1 and LKW 2, the choice of a static initial condition limits the range of solutions available. In the current paper the initial velocity will be arbitrary, enabling us to examine the relative importance of the applied force and the initial momentum of the body and fluid.

It was shown in WLK 1 that the parallel wall geometry leads to a separation of the radial coordinate in the equations of motion. This separation is the time-dependent equivalent of the separation found by Homann (1936) for a steady axisymmetric stagnation-point boundary layer. It is interesting that analogous forms exist for the two-dimensional version of this problem (Secomb 1978) and for the fluid motion in a tube that contracts uniformly along its length (Uchida & Aoki 1977). In each case, there is stagnation flow at the origin of coordinates, the streamwise velocity is proportional to the streamwise coordinate, and the perpendicular velocity is independent of the streamwise coordinate. In all these problems the number of independent variables is reduced by one and the reduced equations lead to exact numerical solutions of the Navier-Stokes equations. Yang (1958) showed that for a time-dependent two-dimensional stagnation-point flow, a further simplification can be obtained if the outer flow has the special dimensionless form

$$u_\infty = \frac{x}{1 - \alpha t}. \quad (1)$$

In this case a similarity solution is found and the number of independent variables is further reduced, so the flow is determined in terms of a function of a single variable. Uchida & Aoki (1977) found that a particular time-dependence of the tube radius also leads to a similarity solution; in fact this also leads to a streamwise velocity like (1). However, these two solutions have no special physical interpretation; the

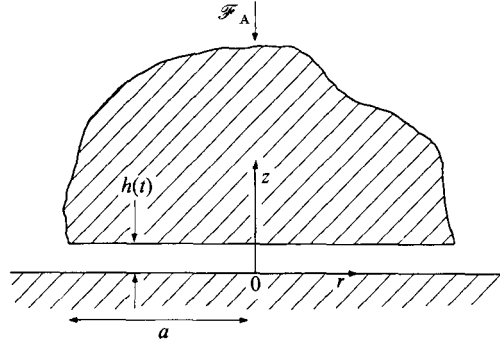


FIGURE 1. The geometry and coordinate system for a flat body near a plane.

time-dependence is introduced artificially as a mathematical convenience in the solution. We will show that a similar solution arises naturally in the present problem and that it has a simple physical interpretation.

When the governing equations are cast in dimensionless form, we find that in the general case there are three dimensionless parameters governing the motion. These are

$$Re_0 = \frac{h_0 |w_0|}{\nu}, \quad \beta = \frac{4mh_0}{\pi\rho a^4}, \quad \gamma = \frac{V_0^2}{w_0^2}, \quad (2)$$

in which  $\nu$  and  $\rho$  are the kinematic viscosity and density of the fluid, and  $m$  and  $w_0$  are the mass and initial velocity of the disk.  $V_0$  is a velocity scale based on the initial gap height and the characteristic inertial time required to drain the fluid under an applied force  $\mathcal{F}_A$  which includes gravity

$$V_0 = \left( \frac{4\mathcal{F}_A}{\pi\rho a^2} \right)^{\frac{1}{2}} \frac{h_0}{a}. \quad (3)$$

The first parameter is the Reynolds number based on the initial gap height, the second parameter is the ratio of the contribution to the dynamic equation of the inertia of the body to that of the inertia of the fluid, and  $\gamma$  is the ratio of the applied force to the pressure force induced by the inertia of the fluid.  $Re_0$  may be very small for microscopic particles or quite large for larger particles (e.g. for a large snowflake hitting a window  $Re_0 \approx 10^3$ ).  $\beta$  is typically  $\ll O(1)$  for liquids and for small gap height, but may be large for solid particles in a gas (e.g. for a penny dropped in a puddle of water  $\beta \approx 10^{-2}$ , but for the snowflake hitting a window  $\beta \approx 10^2$ ). Finally,  $\gamma$  depends on the nature of the problem; if there is no applied force  $\gamma$  is zero, if there is no initial velocity  $\gamma$  is infinite.

The equations of motion will be treated in the inviscid limit for all values of  $\beta$  and  $\gamma$ . In particular when  $\beta$  is large, it will be shown that a large pressure builds up rapidly in the fluid gap. This is very significant for elastic bodies, because a large portion of the kinetic energy could be stored, leading to recoil of the body. For real fluids with finite  $Re_0$ , we shall consider two problems: (a) the near-collision arrest of an object driven solely by inertia in the absence of an applied force and (b) the modification of this flow when an applied force is present, with inertia playing a subsidiary role.

We define a time-dependent Reynolds number, which leads to a single solution curve that is valid for the entire range of Reynolds numbers from the initial value

to zero at final arrest. This solution is divided into three parts. The first part is a boundary-layer solution valid for  $Re_0 > O(100)$  which is an exact similarity solution when  $\beta = 0$ , the second part is a numerical solution for  $O(0.1) < Re_0 < O(100)$  and the third part is a low-Reynolds-number analysis. Amongst other things, this solution predicts the ultimate position of rest of the body in the absence of an applied force.

## 2. Governing equations

The equations of motion for the body and fluid were derived in WLK 1. A slightly different notation is used here but the derivation is not included. The fluid velocity is given by  $u = |w_0| r F_z$ ,  $w = -2|w_0| F$  in terms of a dimensionless stream function  $F(z, t)$  and the initial velocity of the disk  $w_0$ . The initial gap height  $h_0$  is used as a lengthscale, and the timescale is chosen to be  $h_0/|w_0|$ . In dimensionless form, the governing equations are

$$F_{zt} + F_z^2 - 2FF_{zz} - \frac{1}{Re_0} F_{zzz} = \beta h_{tt} + \gamma. \quad (4)$$

$$\text{with} \quad \text{when } t = 0 \quad F = F_0(z), \quad h = 1, \quad h_t = -1, \quad (5)$$

$$\text{on } z = 0 \quad F = 0, \quad F_z = 0, \quad (6)$$

$$\text{on } z = h(t) \quad F_z = 0, \quad h_t = -2F. \quad (7)$$

In many cases, it may be difficult to specify the initial stream function  $F_0(z)$ , but we shall see that a 'natural' form for  $F_0$  is generated in some circumstances.

## 3. Inviscid solution

If the initial Reynolds number is very large, the effects of viscosity will be confined in space to thin boundary layers and in time towards the end of the motion. For a large part of the motion the inviscid equations will give a good representation of the solution. The differential equations (4)–(7) can be satisfied by taking  $F = \Phi(t)z$  to give

$$\Phi_t + \Phi^2 = \beta h_{tt} + \gamma \quad (8)$$

$$\text{with} \quad h_t = -2h\Phi \quad (9)$$

$$h = 1, \quad \Phi = \frac{1}{2} \quad \text{when } t = 0. \quad (10)$$

Equation (10) requires that

$$F_0(z) = \frac{1}{2}z. \quad (11)$$

Now in inviscid flow, the instantaneous stream function is determined uniquely by the boundary conditions, so if the boundary conditions are to hold at the initial instant, then  $F_0$  must have the form of (11). Alternatively, we may regard  $F_0(z)$  as an unknown function which we have determined as part of the solution.

We eliminate  $\Phi$  from (8) using (9) to give

$$\left(\beta + \frac{1}{2h}\right) h_{tt} - \frac{3}{4} \left(\frac{h_t}{h}\right)^2 + \gamma = 0. \quad (12)$$

Equation (12) was derived in WLK 1 with a different scaling so that  $\gamma$  was replaced by unity, and solved subject to the initial conditions  $h = 1$  and  $h_t = 0$ . It was

integrated numerically for representative values of  $\beta$  and an analytic solution was given for  $\beta = 0$  (cf. case (ii) below).

Since (12) does not contain  $t$  explicitly, we can obtain a first integral by introducing  $J(h) = \frac{1}{2}h_t^2$ , so that  $J = dJ/dh = h_{tt}$ . Then we have

$$J' - \frac{3J}{h(1+2\beta h)} = \frac{-2h\gamma}{1+2\beta h}. \tag{13}$$

This equation is of standard form and has the solution

$$J(h) = h^3 \left( \frac{1+2\beta}{1+2\beta h} \right)^3 \left\{ \frac{1}{2} + \frac{2\gamma}{(1+2\beta)^3} \left[ 4\beta^2(1-h) + 4\beta \log \frac{1}{h} + \frac{1}{h} - 1 \right] \right\}. \tag{14}$$

Now  $h_t = -(2J(h))^{\frac{1}{2}}$ , so we have formally

$$t = \int_h^1 [2J(x)]^{-\frac{1}{2}} dx. \tag{15}$$

This integral is not amenable to analytical calculation in the general case, but may be evaluated in the following special cases.

Case (i)  $\gamma = 0, \beta \neq 0$

In this case  $J(h)$  reduces to

$$J(h) = \frac{1}{2}h^3 \left( \frac{1+2\beta}{1+2\beta h} \right)^3. \tag{16}$$

So we have

$$t = \frac{1}{\beta} \left( 1 + \frac{1}{2\beta} \right)^{-\frac{3}{2}} \left[ \left( 1 + \frac{1}{2\beta h} \right)^{\frac{1}{2}} (1-\beta h) - \left( 1 + \frac{1}{2\beta} \right)^{\frac{1}{2}} (1-\beta) - \frac{3}{2} \coth^{-1} \left( 1 + \frac{1}{2\beta h} \right)^{\frac{1}{2}} + \frac{3}{2} \coth^{-1} \left( 1 + \frac{1}{2\beta} \right)^{\frac{1}{2}} \right]. \tag{17}$$

From (9) and (16)  $\Phi$  is given by

$$\Phi = -\frac{1}{2} \frac{h_t}{h} = \frac{1}{2} h^{\frac{1}{2}} \left( \frac{1+2\beta}{1+2\beta h} \right)^{\frac{3}{2}}. \tag{18}$$

Solutions (17) and (18) are shown in figures 2(a) and (b) respectively.

The dimensionless hydrodynamic force on the disk is  $\beta h_{tt}$ , which is proportional to  $\mathcal{F}_H(t)$  and the pressure at the centre of the underside of the disk,  $p_0(t)$ . From (16) we have

$$h_{tt} = J'(h) = \frac{3}{2} h^2 \frac{(1+2\beta)^3}{(1+2\beta h)^4}. \tag{19}$$

The solutions for  $\Phi$  (which is proportional to radial velocity) and  $h_{tt}$  shown in figure 2(b and c) are of particular interest. We see that both  $\Phi$  and  $h_{tt}$  are strongly dependent on  $\beta$ . For small  $\beta$ ,  $h_{tt}$  (or the fluid pressure) decays monotonically as does the radial velocity. For large  $\beta$ , the force is relatively small except for a short time near  $t = 1$ , when the body is rapidly brought to a stop by a very large force, which approaches a unit impulse as  $\beta \rightarrow \infty$ . The force comes from the large pressure generated under the body by the large radial velocities which arise as the gap

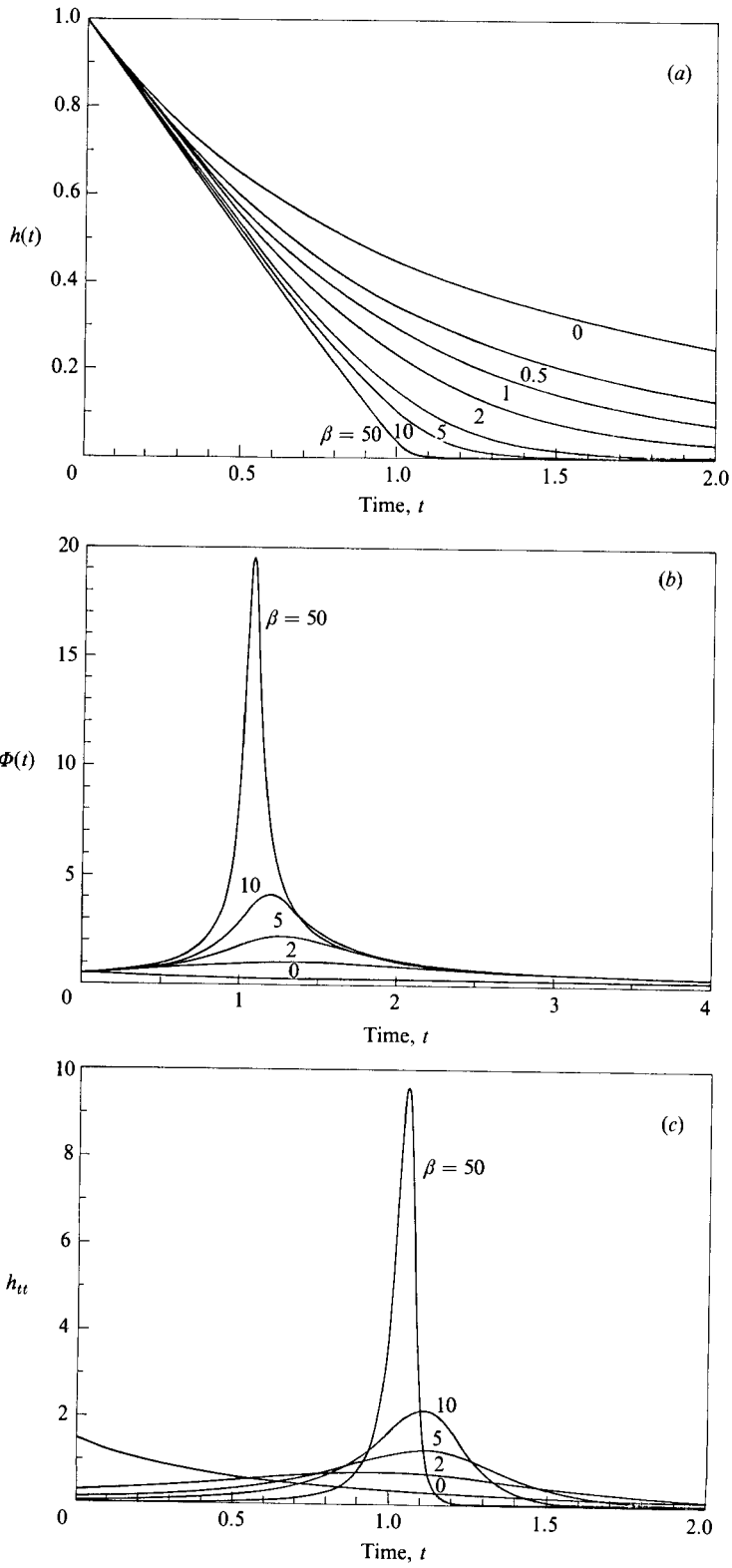


FIGURE 2. Inviscid solutions case (i)  $\gamma = 0$ : (a)  $h(t)$ , (b)  $\Phi(t)$ , (c)  $h_{tt}$ .

becomes very narrow. This is evident from the comparison of the  $\beta = 50$  curves in figure 2(b and c) where the maxima of the  $h_{tt}$  and  $\Phi$  curves are coincident. If (8) is multiplied by  $h_t$ , the right-hand side is immediately recognized as the time derivative of the kinetic energy of the body; the time integral of this term is the work done by the body in transferring its own kinetic energy to the surrounding fluid. When  $\beta$  is small, most of the kinetic energy is contained in the fluid which has a chance to escape at the edge of the body and there is only a minor transfer of kinetic energy to the fluid in the gap before final arrest. For large  $\beta$ , however, the escaping fluid contains only a small portion of the total kinetic energy with the result that very large accelerations and dynamic pressures can be built up in the near collision or impact region. This behaviour has important implications for the collision and recoil of an elastic body which are discussed in the concluding section.

*Case (ii)  $\beta = 0, \gamma \neq 0$*

In this case the equation for  $\Phi$ , (8), becomes decoupled from  $h$ , so it is easier to proceed directly. This problem has different solutions depending on the value of  $\gamma$ .

$$\text{If } \gamma = \frac{1}{4}, \text{ then } \Phi = \frac{1}{2}. \tag{20}$$

$$\text{If } \gamma < \frac{1}{4}, \text{ then } \Phi = \gamma^{\frac{1}{2}} \coth [\gamma^{\frac{1}{2}}(t+c)] \tag{21}$$

$$\text{with } c = \gamma^{-\frac{1}{2}} \coth^{-1}(4\gamma)^{-\frac{1}{2}}. \tag{22}$$

$$\text{If } \gamma > \frac{1}{4}, \text{ then } \Phi = \gamma^{\frac{1}{2}} \tanh [\gamma^{\frac{1}{2}}(t+c)] \tag{23}$$

$$\text{with } c = \gamma^{-\frac{1}{2}} \tanh^{-1}(4\gamma)^{-\frac{1}{2}}. \tag{24}$$

We use (9) to find the respective solutions for  $h$ :

$$\gamma = \frac{1}{4}, \quad h = e^{-t}, \tag{25}$$

$$\gamma < \frac{1}{4}, \quad h = \frac{\operatorname{cosech}^2 [\gamma^{\frac{1}{2}}(t+c)]}{\operatorname{cosech}^2 (c\gamma^{\frac{1}{2}})}, \tag{26}$$

$$\gamma > \frac{1}{4}, \quad h = \frac{\operatorname{sech}^2 [\gamma^{\frac{1}{2}}(t+c)]}{\operatorname{sech}^2 (c\gamma^{\frac{1}{2}})}. \tag{27}$$

These solutions for  $h$  and  $\Phi$  are shown in figure 3(a, b). Comparison of figures 2(a, b) and 3(a, b) clearly shows the difference between draining behaviour under a force due to body inertia and a constant applied force such as gravity. For a constant applied force with  $\gamma > \frac{1}{4}$  the radial velocity asymptotically approaches a constant value for which the dynamic pressure force in the fluid gap just balances the applied force. The radial velocity cannot, therefore, exhibit a local maximum as a function of time, nor can there be a pressure overshoot when  $\beta = 0$ .

*Case (iii)  $\beta = 0, \gamma = 0$*

This is the simplest case of all; we immediately find

$$\Phi = \frac{1}{t+2}. \tag{28}$$

and 
$$h = \frac{4}{(t+2)^2} = 4\Phi^2. \tag{29}$$

These results are included in figures (2) and (3).

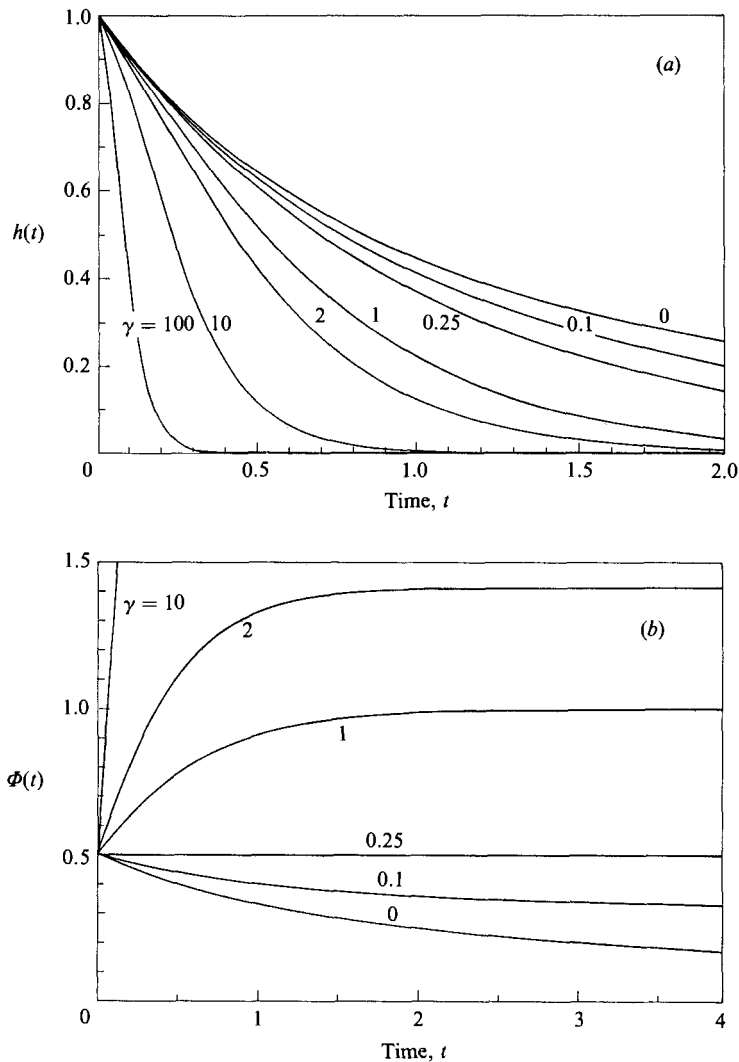


FIGURE 3. Inviscid solutions case (ii)  $\beta = 0$ : (a)  $h(t)$ , (b)  $\Phi(t)$ .

#### 4. Solution procedure for the viscous case

There are two main problems of interest in solving (4). The first is the hydrodynamic arrest by viscous dissipation of a moving body approaching a solid boundary, where the driving force for the motion is the initial momentum of the body and fluid. The second problem is that of complete draining of the fluid in the gap under the action of a constant applied force. The solution procedure for these two problems is outlined below.

##### 4.1. Hydrodynamic arrest

The body will come to rest before reaching the plane only if there is no applied force, i.e. we must take  $\gamma = 0$ . We are left with a two-parameter family of solutions for different values of  $\beta$  and  $Re_0$ . The initial stream function  $F_0(z)$  is unknown, but it must reflect the previous history of the motion and the instantaneous Reynolds



number based on gap height when the solution is started. If  $Re_0$  and the initial gap height are large, we would expect  $F_0(z)$  to be very close to the inviscid solution found in §3, except for the presence of thin boundary layers on the top and bottom walls. On the other hand, for smaller values of  $Re_0$  we would expect the velocity profile  $F_{0z}$  to be more or less parabolic. We consider for the moment the solution for a given value of  $\beta$  and a large  $Re_0$ . On physical grounds, we expect both the dimensionless gap height  $h$  and the descent rate  $|h_t|$  to decrease monotonically as the motion progresses. We can define a time-dependent Reynolds number,  $Re(t) = Re_0 h |h_t|$ , which will decrease monotonically from  $Re_0$  to zero during the motion. When  $Re_0$  is very large we could, for example, choose the inviscid flow as a realistic initial condition, but when  $Re_0$  is not large, the form of the initial condition is not obvious. However, a suitable candidate is available in the form of the instantaneous solution for large  $Re_0$  at the appropriate time when  $Re(t)$  has the desired value. This solution will be a good choice for the initial stream function provided that it is independent of the large value used for  $Re_0$ . In this way, the solution exhibits a similarity behaviour in which the initial profile depends on  $Re_0$ .

The above argument provides us with two benefits. First, the initial condition chosen for the stream function is, in a sense, the most natural one. Secondly, we need only *one* solution of the problem to cover the whole range of  $Re_0$  at a given  $\beta$ . To obtain the solution for smaller  $Re_0$ , we simply discard the portion of the solution with  $Re(t) > Re_0$  and rescale the remaining portion of the motion to give unit initial conditions.

#### 4.2. *Draining under a constant force*

When a force is applied, the body will not come to rest until it is in contact with the plane, a process which takes an infinite time. There are two cases which are of particular interest: (i) the body is dropped from rest, and (ii) the body arrives from 'far away' with non-zero initial velocity. In both cases, the velocity scale is determined by the applied force, so we use the velocity scale  $V_0$  given by (3). If we redefine the Reynolds number so that  $\overline{Re}_0 = Re_0 \gamma^{\frac{1}{2}} = h_0 V_0 / \nu$  and define  $\overline{w}_0 = -\gamma^{-\frac{1}{2}}$ , then we have

$$F_{zt} + F_z^2 - 2FF_{zz} - \frac{F_{zzz}}{\overline{Re}_0} = \beta h_{tt} + 1, \tag{30}$$

where  $h = 1, \quad h_t = \overline{w}_0, \quad F = F_0(z) \quad \text{at } t = 0. \tag{31}$

Equation (30) is the same as (4) with  $\gamma = 1$ . The only difference is in the initial value of  $h_t$ . It is clear then that, by replacing  $\gamma$  by zero or unity in (4), we can solve the two problems of major interest, provided we allow a little more flexibility in the initial value of  $h_t$ . Thus we do not need to consider arbitrary values of  $\gamma$  in (4).

In case (i) when the body is dropped from rest, both  $\overline{w}_0$  and  $F_0(z)$  are zero. The solution of (30) is essentially different for each combination of  $\overline{Re}_0$  and  $\beta$ , so the full two-parameter family of solutions is needed. This case was the basis of the studies in WLK 1 and LKW 2 and we shall not discuss it further.

In case (ii) the initial condition is unspecified and, as in §4.1 above, we must find the initial stream function as part of the solution; we must also find the appropriate value of  $\overline{w}_0$ . The time-dependent Reynolds number for this problem is  $\overline{Re}(t) = \overline{Re}_0 h^2(t)$ , since  $V_0$  is proportional to  $h_0$ . The behaviour is qualitatively the same as that for the problem in §4.1 and the same method of solution may be applied. For a given value of  $\beta$ , we take  $\overline{Re}_0$  to be very large and use the inviscid solution as the initial condition. The sequence of states with smaller  $\overline{Re}(t)$  then gives the initial conditions

for each smaller value of  $\overline{Re}_0$ . Again only one solution of the problem is needed to cover the whole range of  $\overline{Re}_0$  for a given  $\beta$ .

The solution method outlined above enables us to simplify the range of parameters and starting conditions for the solution. Instead of a three-parameter family of solutions with unknown initial conditions, we only need to find two one-parameter families of solutions for the two problems of §§4.1 and 4.2. The extra degrees of freedom have been removed by choosing the most convenient (and realistic) initial conditions. In addition, the equations for  $F$  and  $h$  decouple when  $\beta = 0$ . This will enable us to find new boundary-layer-type similarity solutions to the Navier–Stokes equations in which the inviscid outer flow has a meaningful physical interpretation. This simplification is not possible for non-zero  $\beta$ ; in this case the solutions require much more numerical computation, so we shall only present results for  $\beta = 0$ .

In LKW 2, it was indicated that the similarity boundary-layer solution for the problem of §4.2 is simply a steady stagnation-point flow, because the inviscid core flow is constant (cf. (20)). Since the solution is so simple and the methods are contained in those for the problem of §4.1, WLK 1 and LKW 2, the calculations will not be shown here. Graphical results will be presented at the end of the following section for comparison with the problem of §4.1.

## 5. Hydrodynamic arrest with small $\beta$

As discussed earlier, the parameter  $\beta$  represents the ratio of the forces due to the inertia of the body to those due to the inertia of the fluid. It might, therefore, appear unreasonable to consider the case  $\beta = 0$  for hydrodynamic arrest because if we neglect both the inertia of the body and the applied force there is no apparent forcing in the problem. However, if the gap is sufficiently small, the fluid within it may have a large radial velocity so that the momentum possessed by the fluid at the initial instant is much larger than that of the body which is moving much more slowly in the axial direction. Thus, the forcing in the problem comes from the initial conditions and there is no contradiction in examining the limit  $\beta = 0$ .

The solution of this problem has three components – an exact similarity boundary-layer solution for large  $Re_0$  or  $Re(t)$ , a numerical solution for intermediate  $Re_0$  or  $Re(t)$  and a low-Reynolds-number solution.

### 5.1. Boundary-layer solution

The ‘outer’ inviscid flow is given by

$$F = (z - \delta(t)) \Phi(t), \quad (32)$$

with  $\delta(t)$  defined by

$$\delta(t) = \int_0^{h/2} \left( 1 - \frac{F_z}{\Phi} \right) dz. \quad (33)$$

$\Phi(t)$  satisfies (8) with  $\beta$  and  $\gamma$  equal to zero, cf. (28), whose solution is

$$\Phi = \frac{1}{t + c_1}, \quad (34)$$

in which  $c_1$  is an arbitrary constant to be determined from the initial condition. The boundary-layer scaling is  $F = Re_0^{-\frac{1}{2}} f(\zeta, t)$  with  $\zeta = Re_0^{\frac{1}{2}} z$ . Equations (4)–(7) are replaced by

$$f_{\zeta\zeta} + f_{\zeta}^2 - 2ff_{\zeta\zeta} - f_{\zeta\zeta\zeta} = 0, \quad (35)$$

where  $f = 0, \quad f_\zeta = 0 \quad \text{on } \zeta = 0,$  (36)

$$f_\zeta \sim \Phi(t) \quad \text{as } \zeta \rightarrow \infty, \tag{37}$$

$$f = f_0(\zeta) \quad \text{when } t = 0. \tag{38}$$

Equations (35)–(38) describe a time-dependent axisymmetric stagnation-point boundary-layer flow which is analogous to the two-dimensional form studied by Yang (1958). The particular form of  $\Phi$  (34) allows us to find a time-dependent similarity scaling:

$$f = \Phi^{\frac{1}{2}} g(\eta) \quad \text{with } \eta = \Phi^{\frac{1}{2}} \zeta. \tag{39}$$

Then we derive the similarity problem:

$$g''' + 2gg'' - g'^2 + \frac{1}{2}\eta g'' + g' = 0, \tag{40}$$

where  $g = 0, \quad g' = 0 \quad \text{on } \eta = 0$  (41)

and  $g' \rightarrow 1 \quad \text{as } \eta \rightarrow \infty.$  (42)

We define the number  $d$  by

$$d = \int_0^\infty (1-g') d\eta = \lim_{\eta \rightarrow \infty} (\eta - g) = 0.601\,159. \tag{43}$$

Then  $\delta = Re_0^{-\frac{1}{2}} \Phi^{-\frac{1}{2}} d.$  (44)

The equation for  $h(t)$  becomes

$$h_t + 2h\Phi = 4\delta\Phi = 4d Re_0^{-\frac{1}{2}} \Phi^{\frac{1}{2}}. \tag{45}$$

This has the solution

$$h = \frac{c_2}{(t+c_1)^2} + \frac{8}{5}d Re_0^{-\frac{1}{2}} (t+c_1)^{\frac{1}{2}} = c_2 \Phi^2 + \frac{8}{5}\delta. \tag{46}$$

We now apply initial conditions (5) to  $h$  to get

$$c_1^\pm = 2 + \frac{8d^2}{Re_0} \pm 4\sqrt{2d Re_0^{-\frac{1}{2}} \left(1 + \frac{2d^2}{Re_0}\right)^{\frac{1}{2}}} \tag{47}$$

and  $c_2 = \frac{1}{5}c_1^2(1+2c_1).$  (48)

For large  $Re_0$ , we have  $c_1^\pm \approx 2, c_2 \approx 4$ . To find the correct sign for  $c_1$  in (47), we use (34) and (45) to obtain

$$\Phi(0) = 1/c_1 = h_t(0)/(4\delta(0) - 2h(0)) = 1/(2 - 4\delta(0)). \tag{49}$$

This shows that  $c_1 = 2 - 4\delta(0) < 2$ , so we choose  $c_1 = c_1^-$ .

The apparently difficult time-dependent boundary-layer problem has been greatly simplified by the use of ‘natural’ initial conditions. The above solution is exact whenever there are distinct boundary layers. The function  $g'$  is within  $10^{-8}$  of unity at  $\eta = 4$  and it is convenient to take this as the edge of the boundary layer. At the time when  $\eta = 4$  corresponds to  $z = \frac{1}{2}h$ , we have  $4 = \Phi^{\frac{1}{2}} Re_0^{\frac{1}{2}} \frac{1}{2}h$ , i.e.  $Re_0 \Phi h^2 = 64$ . Now for large  $Re(t)$ ,  $h_t \approx -2h\Phi$ , so  $Re(t) \approx 2Re_0 \Phi h^2$ . Hence the boundary-layer solution is valid whenever  $Re(t) > 128$ . This estimate is very conservative and the solution is still quite accurate at lower Reynolds numbers.

## 5.2. Numerical solution

We take  $Re_0 = 128$  and use the boundary-layer solution to (40)–(42) as the initial condition. First, (40) for  $g(\eta)$  is integrated up to  $z = 1$  using a shooting method with interval halving to find  $g''(0)$  and a fifth-order Runge–Kutte–Verner method of integration. To avoid large errors at the symmetry boundary  $z = \frac{1}{2}$ , the derivative of the stream function is taken to be  $F_z(z)F_z(1-z)$ , with  $z = [Re_0\Phi(0)]^{-\frac{1}{2}}\eta$ .

The moving boundary is inconvenient for numerical integration and we introduce a new scaled coordinate  $x = z/h(t)$  which is constant at  $z = h$ . We also define a scaled velocity  $U = F_z = F_x/h$  whose time derivative is

$$U_t = \frac{U_{xx}}{Re_0 h^2} + \frac{U_x h_t x}{h} + \frac{2FU_x}{h} - U^2. \quad (50)$$

The boundary conditions in terms of these new scaled variables are

$$F = 0, \quad U = 0 \quad \text{on } x = 0, \quad (51)$$

$$U_x = 0, \quad h_t = -4F \quad \text{on } x = \frac{1}{2}. \quad (52)$$

The space dimension is now discretized so that  $x$  is restricted to the values  $x_I, I = 1, \dots, n$  with  $x_1 = 0, x_{n-1} = 0.5$  and  $x_I - x_{I-1} = \Delta x = 0.5/(n-2)$ . It is advantageous to choose  $n-2 = 2^m$ , so that  $\Delta x$  may be doubled without needing to interpolate. For our problem  $n = 130$  was adequate to keep the error below  $10^{-5}$ . The discretization leaves a set of  $n+1$  ordinary differential equations for  $U_I$  and  $h$ . We represent the derivatives of  $U$  and  $F$  by finite differences accurate up to  $O(\Delta x^4)$  and then explicitly evaluate the  $\Delta x^4$  terms to give a conservative estimate of the error. When the estimated error is very small, the space step  $\Delta x$  can be doubled to speed up the integration. Equations (50)–(52) rewritten in the discretized variables are integrated forward in time as far as is necessary using the aforementioned Runge–Kutte–Verner method.

The truncation and integration errors for each time derivative are controlled to a relative magnitude of  $10^{-5}t$  until the absolute value falls below  $10^{-2}t$  when an absolute error of  $10^{-7}t$  is allowed. This estimate is very conservative, so the results can be regarded as very accurate. In fact, the integration need only be carried up to moderate values of  $t$ , since then  $Re(t)$  is very small, and the low-Reynolds-number analytic theory described next can be applied.

## 5.3. Low-Reynolds-number solution

The long viscous timescale  $Re_0 t$  used in WLK1 is inappropriate for this problem since there is no forcing and the flow would be identically zero. In the low-Reynolds-number limit, the inertial forces are tiny, so this part of the motion is just a rapid deceleration to zero flow, i.e. the actual arrest of the body. We introduce a short timescale  $t = Re_0 \tau$ . Then we have

$$F_{zzz} - F_{z\tau} = Re_0 (F_z^2 - 2FF_{zz}), \quad (53)$$

with 
$$F = 0, \quad F_z = 0 \quad \text{on } z = 0, \quad (54)$$

$$F_z = 0, \quad h_\tau = -2Re_0 F \quad \text{on } z = h(\tau), \quad (55)$$

$$h = 1, \quad h_\tau = -Re_0, \quad F = F_0(z) \quad \text{when } \tau = 0. \quad (56)$$

A suitable form for  $F_0(z)$  is to be determined. We notice that  $h_\tau$  is small, so  $h$  will remain close to unity and therefore pose asymptotic expansions of the form

$$h(\tau; Re_0) \sim 1 + Re_0 \tilde{h}_1(\tau) + Re_0^2 \tilde{h}_2(\tau), \tag{57}$$

$$F(z, \tau; Re_0) \sim \tilde{F}_0(z, \tau) + Re_0 \tilde{F}_1(z, \tau) + Re_0^2 \tilde{F}_2(z, \tau). \tag{58}$$

The zero-order problem is

$$\tilde{F}_{0zzz} - \tilde{F}_{0z\tau} = 0, \tag{59}$$

where 
$$\tilde{F}_0 = 0, \quad \tilde{F}_{0z} = 0 \quad \text{on } z = 0 \tag{60}$$

and 
$$\tilde{F}_{0z} = 0 \quad \text{on } z = 1. \tag{61}$$

The boundary condition has been ‘moved’ to  $z = 1$  by expanding in a Taylor series about  $z = 1$ . The general solution to (59)–(61) is

$$\tilde{F}_0 = \sum_1^\infty a_n (1 - \cos n\pi z) e^{-n^2\pi^2\tau}. \tag{62}$$

The  $a_n$  are to be determined from the initial condition. The solution is very strongly damped and after a short while it will be dominated by the leading term. Hence the ‘natural’ initial condition is

$$\tilde{F}_0 = a_1 (1 - \cos \pi z) \quad \text{when } \tau = 0, \tag{63}$$

and the solution is then

$$\tilde{F}_0 = a_1 (1 - \cos \pi z) e^{-\pi^2\tau}. \tag{64}$$

The first-order problem for  $h$  is

$$\tilde{h}_{1\tau} = -2\tilde{F}_0 \quad \text{on } z = 1 \tag{65}$$

$$= -4a_1 e^{-\pi^2\tau}. \tag{66}$$

Thus

$$\tilde{h}_1 = -\frac{4a_1}{\pi^2} (1 - e^{-\pi^2\tau}). \tag{67}$$

The second initial condition is

$$\tilde{h}_{1\tau} = -1 \quad \text{when } \tau = 0. \tag{68}$$

Therefore we have

$$a_1 = \frac{1}{4}. \tag{69}$$

The next-order problem is

$$\tilde{F}_{1zzz} - \tilde{F}_{1z\tau} = \tilde{F}_{0z}^2 - 2\tilde{F}_0 \tilde{F}_{0zz}, \tag{70}$$

with 
$$\tilde{F}_1 = 0, \quad \tilde{F}_{1z} = 0 \quad \text{on } z = 0, \tag{71}$$

$$\tilde{F}_{1z} + \tilde{h}_1 \tilde{F}_{0zz} = 0 \quad \text{on } z = 1. \tag{72}$$

The forcing in (70) has time-dependence  $e^{-2\pi^2\tau}$  which is very strongly damped. Hence the only important contribution is of the same form as (64), forced by the  $(1 - \cos \pi z)$ -term in the initial condition and by (72). However, we can arrange that this term is zero by absorbing any contribution into the zero-order solution. Hence we can neglect the first- and higher-order corrections to  $F$ . Thus, we have

$$h = 1 - \frac{1}{\pi^2} (1 - e^{-\pi^2\tau}) Re_0 + O(Re_0^2), \tag{73}$$

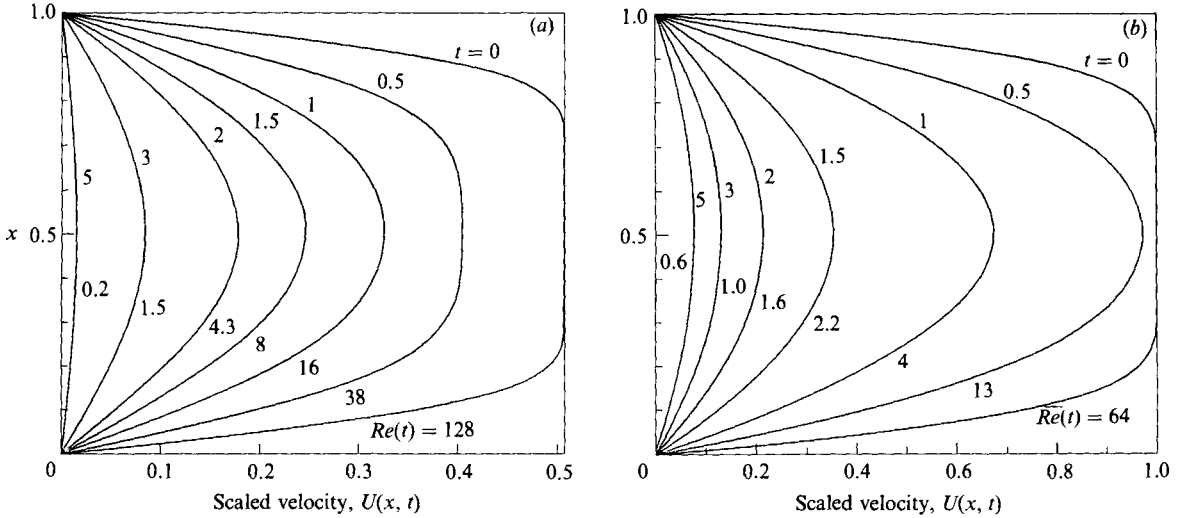


FIGURE 4. Viscous evolution of velocity profiles with  $\beta = 0$ : (a) motion driven by inertia §4.1, (b) constant applied force §4.2.

and the final position of the disk is given by

$$h_\infty = 1 - \frac{1}{\pi^2} Re_0 + O(Re_0^2). \tag{74}$$

It seems that the numerical coefficients will become smaller with increasing powers of  $Re_0$ , so we may estimate the error in (74) as roughly  $\frac{1}{10} Re_0^2$ . Then we have five-figure accuracy provided  $Re_0 \leq 10^{-2}$ . Hence the numerical calculation must be continued until  $Re(t) = 10^{-2}$ . This occurs at  $t \approx 8.5$ .

An unusual feature of the above solution is that the velocity profile ultimately takes on the shape of a half sine wave rather than the more usual parabolic form which occurs in the problem of §4.2 where the fluid drains under a constant applied force. The evolution of the velocity profiles from boundary-layer-type to low Reynolds numbers is shown in figure 4(a, b); the most noticeable difference is that the inviscid core flow decays with time in the problem of §4.1, whereas it is constant in the problem of §4.2 where the velocity decay is caused solely by the overlap of the viscous boundary layers.

The effect of  $Re_0$  or  $\overline{Re}_0$  on the descent of the body is shown in figure 5(a, b). Each figure is obtained from a single solution curve (for  $Re_0$  or  $\overline{Re}_0 = 10^6$ ) which is rescaled to give several different values of  $Re_0$  or  $\overline{Re}_0$ . It is clear that all the curves in figure 5(b) asymptote to zero, since the applied force will ultimately drain all the fluid. When there is no applied force, the body is arrested away from the plane, and this is clearly shown in figure 5(a). The matching of the three phases of solution §§5.1, 5.2, 5.3 is shown in figure 6(a, b). This matching is very good for the problem of §4.2 with a constant force, the numerical phase of solution being virtually unnecessary. The deviation from boundary-layer-type behaviour is much more rapid in the problem of §4.1 since the velocity decays rapidly as inertia is overcome by viscosity. Finally, figure 7 shows the position of rest for the problem of §4.1,  $h_\infty$ , as a function of  $Re_0$ . At low Reynolds number, the motion is rapidly damped and the body hardly moves, whilst for large  $Re_0$ , the inertia carries the body close to the plane before viscous forces take over.

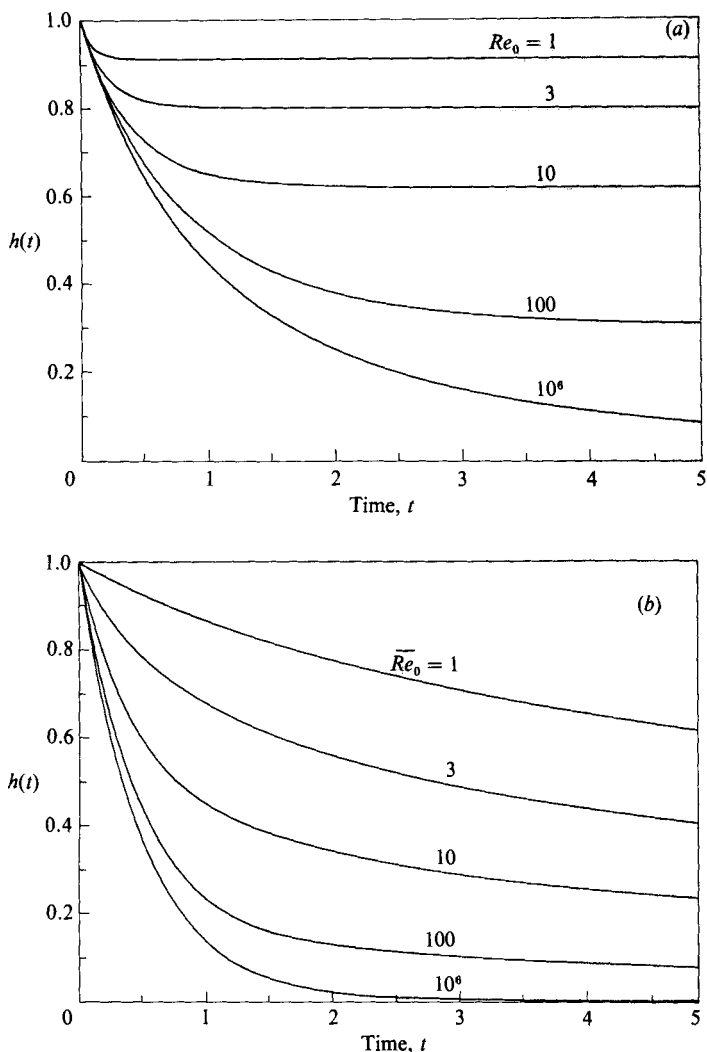


FIGURE 5. (a) The effect of  $Re_0$  on the arrest process. (b) The effect of  $\overline{Re}_0$  on the draining process.

### 6. Concluding remarks

Equation (4) contains three parameters  $Re_0$ ,  $\beta$  and  $\gamma$ , and we have indicated the solution procedure for every regime. Numerical results have been presented in the inviscid limit  $Re_0 \rightarrow \infty$  for either  $\gamma = 0$  or  $\beta = 0$ , and for viscous fluids only for the limiting case  $\beta \rightarrow 0$ . The inviscid results clearly indicate that for  $\beta \neq 0$  the finite- $Re_0$  solutions will depart substantially from the curves in figures 4-7. The effect of viscosity on the solutions of §3 would be to slow the descent rate in general and to damp the singular behaviour for large- $\beta$  observed in the solutions for  $\Phi$  and  $h_{tt}$  in figure 2(b, c). In the case  $\gamma = 0$ , the viscous forces would cause the premature arrest of the body before contact as explained in §4. For large- $\beta$  the inertia of the body provides an important source of energy which must be dissipated by viscous stresses before the body comes to rest. The dramatic acceleration of the core flow shown in figure 2(b) is in sharp contrast to the decelerating core flow of figure 4(a). At high

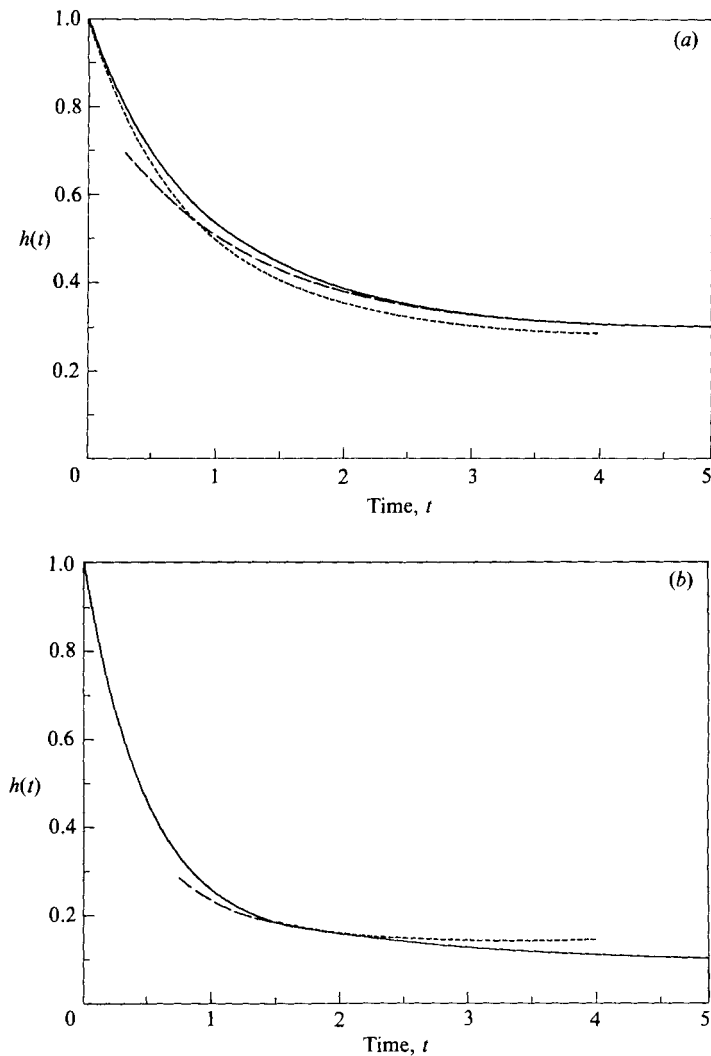


FIGURE 6. Showing the matching of solution phases: §5.1 (.....); §5.2 (—); §5.3 (---)  
 (a) The problem of §4.1,  $Re_0 = 128$ . (b) The problem of §4.2,  $Re_0 = 64$ .

initial Reynolds number and large  $\beta$  the rapid acceleration of the core flow would still occur, leading to the equivalent of the start-up boundary layers that result from impulsively started motions in pipe and channel flows. The subsequent rapid deceleration of the fluid in the core would lead to a complicated overshoot in the boundary-layer velocity profile and probable instability. At lower initial Reynolds number, the effects of viscosity would be felt more quickly; the acceleration of the core flow would be damped and the increase in gap pressure would be diminished.

Real impact problems are further complicated by the elastic deformation of the boundaries which can lead to a damped oscillation of the body after near contact as discussed by Davis *et al.* (1986). In the latter theory, which is based on a viscosity-dominated lubricating-layer analysis, the inertia of the fluid is neglected and thus there can be no transfer of kinetic energy from the body to the fluid in the gap as observed in figure 2(b, c). A large inviscid pressure loading in the near-contact region



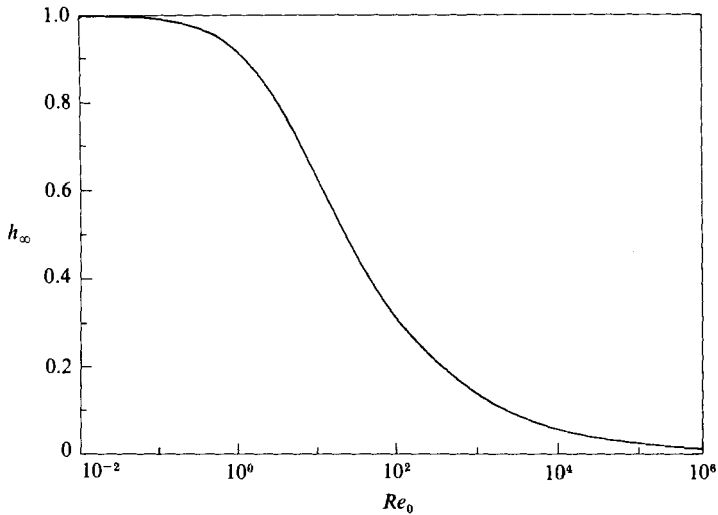


FIGURE 7. The ultimate gap height  $h_\infty$  as a function of  $Re_0$ .

cannot develop and the energy of elastic deformation is completely dissipated by the viscous stresses in the fluid layer. The body is incapable of rebound in this viscosity dominated limit. In contrast, if the pressure loading leading to elastic deformation is largely of an inviscid nature (the high- $Re_0$ , large- $\beta$  case just discussed), the viscous dissipation will not absorb all the elastic recoil energy and the body should be capable of rebound. This more complicated problem is currently under study.

This research was performed in partial fulfillment of the requirements for the Ph.D. degree of C. J. Lawrence from the City University of New York.

#### REFERENCES

- DAVIS, R. H., SERAYSSOL, J.-M. & HINCH, E. J. 1986 The elastohydrodynamic collision of two spheres. *J. Fluid Mech.* **163**, 479.
- HOMANN, F. 1936 Der Einfluss grosser Zähigkeit bei der Strömung um den Zylinder und um die Kugel. *Z. angew. Math. Mech.* **16**, 153.
- LAWRENCE, C. J., KUANG, Y. & WEINBAUM, S. 1985 The inertial draining of a thin fluid layer between parallel plates with a constant normal force. Part 2. Boundary layer and exact numerical solutions. *J. Fluid Mech.* **156**, 479.
- SECOMB, T. W. 1978 Flow in a channel with pulsating walls. *J. Fluid Mech.* **88**, 273.
- UCHIDA, S. & AOKI, H. 1977 Unsteady flows in a semi-infinite contracting or expanding pipe. *J. Fluid Mech.* **82**, 371.
- WEINBAUM, S., LAWRENCE, C. J. & KUANG, Y. 1985 The inertial draining of a thin fluid layer between parallel plates with a constant normal force. Part 1. Analytic solutions; inviscid and small but finite Reynolds number limits. *J. Fluid Mech.* **156**, 463.
- YANG, K.-T. 1958 Unsteady laminar boundary layers in an incompressible stagnation flow. *Trans. ASME E: J. Appl. Mech.* **25**, 421.